

Manuscript

1

2
3 An upgraded drift-diffusion model for evaluating the carrier lifetimes in
4 radiation-damaged semiconductor detectors.5 J. Garcia Lopez*^{1,2}, M. C. Jimenez-Ramos², M. Rodriguez-Ramos², J. Forneris³ and J. Ceballos⁴.
67 ¹Dept of Atomic, Molecular and Nuclear Physics. University of Sevilla. Av. Reina Mercedes s/n.
8 41012 Sevilla, Spain9 ²CNA (U. Sevilla, J. Andalucia, CSIC), Av. Thomas A. Edison 7, 41092 Sevilla, Spain10 ³Physics Dept./NIS Centre, University of Torino, and INFN-Sez. di Torino via P. Giuria 1, 10125
11 Torino, Italy12 ⁴Institute of Microelectronics of Seville, IMSE-CNM (CSIC/University of Seville), Seville 41092,
13 Spain
1415
16 *e-mail: fjl@us.es
1718 The transport properties of a series of n- and p-type Si diodes have been studied by the Ion Beam
19 Induced Charge (IBIC) technique using a 4 MeV proton microbeam. The samples were irradiated
20 with 17 MeV protons at fluences ranging from 1×10^{12} to 1×10^{13} p/cm² in order to produce a uniform
21 profile of defects with depth. The analysis of the charge collection efficiency (CCE) as a function of
22 the reverse bias voltage has been carried out using an upgraded drift-diffusion (D-D) model which
23 takes into account the possibility of carrier recombination not only in the neutral substrate, as the
24 simple D-D model assumes, but also within the depletion region. This new approach for calculating
25 the CCE is fundamental when the drift length of carriers cannot be considered as much greater than
26 the thickness of the detector due to the ion induced damage. From our simulations, we have
27 obtained the values of the carrier lifetimes for the pristine and irradiated diodes, which have allowed
28 us to calculate the effective trapping cross sections using the one dimension Shockley-Read-Hall
29 model. The results of our calculations have been compared to the data obtained using a recently
30 developed Monte Carlo code for the simulation of IBIC analysis, based on the probabilistic
31 interpretation of the excess carrier continuity equations.
32
3334
35 **Keywords:** Drift-diffusion model, semiconductor detector, Ion beam induced charge, Monte Carlo
36 method.
37
38
39
40
41
42
43
44
45
46
47
48
49
50
51
52
53
54
55
56
57
58
59
60
61
62
63
64
65

Introduction

Since its development in the early 1990's [1], the ion beam induced charge (IBIC) technique has found widespread applications to measure and study the transport properties of semiconductor materials and devices [2]. Different theoretical frames have been developed for calculating the charge pulse signal produced by semiconductor detectors. Those models include the use of TCAD simulations [3], the solution of an adjoint carrier continuity equation [4], or the implementation of a simple one-dimensional charge transport by drift and diffusion [5]. In this paper, the drift-diffusion model is revisited to consider the possibility of carrier recombination not only in the electroneutral part of the detector, as stated in [5], but also in the depletion region. The results are applied to a series of Si diodes subjected to radiation damage produced by high energy protons. The present work has been done in the framework of the IAEA Coordinated Research Project F11016 "Utilization of ion accelerators for studying and modeling of radiation induced defects in semiconductors and insulators"

Experimental

The samples studied in this work consist of 300 μm thick n- and p-type Floating Zone Si diodes with doping concentration of $\sim 10^{12}/\text{cm}^3$ fabricated by the Helsinki Institute of Physics (HIP). Fig. 1 shows a scheme of a p-type diode with the doping profile (red line) extracted from the C-V curve determined at the Sandia National Laboratories (SNL) [6]. The inset represents the width of the depletion region vs. reverse bias voltage, as found out in [6].

The irradiations were carried out at the external beam of the compact cyclotron of the CNA, placing the samples in air at 15 cm from the 150 μm thick kapton exit window. Although the cyclotron delivers 18 MeV protons, the actual proton energy at the sample's surface after traversing the kapton foil and the air was 17 MeV, as calculated using the SRIM code [7]. The homogeneous proton beam ($\text{O}=15$ mm) was partially blocked with a 2 mm thick graphite collimator ($\text{O}=10$ mm), which was connected to a Brookhaven 1000c current integrator for fluence measurements. A second collimator made of 2 mm thick Al ($\text{O}=200$ μm) was placed in front of the diode to limit the damaged volume, which otherwise would increase the leakage current to unacceptable values after the irradiation. The diodes were irradiated at fluences between 1×10^{12} p/cm² and 1×10^{13} p/cm².

The study of the defects was accomplished at the microbeam line of the 3MV Tandem accelerator of the CNA, approximately one week after irradiation, with the samples stored at room temperature. IBIC analysis was performed with a 4.07 MeV proton beam, whose ionization profile in Si, as evaluated by SRIM code, is superimposed to the doping profile in Fig. 1 (black line). To avoid creating additional damage during the measurements, the

beam was slightly focused to a spot of $10 \times 10 \mu\text{m}^2$ and the proton rate was kept below 200 Hz. First, the damaged areas were localized through the $1 \times 1 \text{ mm}^2$ IBIC mappings, as shown in Fig. 2, and then point measurements were performed in the center of the perturbed regions to extract the data. The signal height was recorded as a function of the applied bias voltage using a Canberra 2003BT preamplifier, a Tennelec TC245 amplifier with a shaping time of $2 \mu\text{s}$ and the OMDAQ ADC/MCA system from Oxford Microbeams Ltd. A triple alpha source (^{244}Cm , ^{241}Am and ^{239}Pu) with about $1 \mu\text{Ci}$ activity was placed inside the vacuum chamber. In that way the alpha spectrum was simultaneously recorded together with the IBIC signals providing an absolute calibration of the full electronic chain. Moreover, in order to correct for the possible changes in the overall electronic gain due to the variation of the detector capacitance at different bias, a calibrated pulser was connected to the “Test” input of the preamplifier. No significant changes in the position of the pulser signal for bias voltages between 42 V and 0.5 V were observed during the measurements.

Calculation of the measured charge collection efficiency

As shown by M. Breese in his pioneer paper about the theory of ion beam induced charge collection [5], the measured (normalised) charge collection efficiency (CCE) can be expressed in a partially depleted device as:

$$CCE = CCE_{Drift} + CCE_{Diffusion} = \frac{1}{E_i} \left(\int_0^w \frac{dE}{dx} dx + \int_w^{R_p} \frac{dE}{dx} e^{-\frac{x-w}{L_{diff}}} dx \right) \quad (1)$$

where E_i , R_p and dE/dx are the initial energy, the projected range and the ionizing energy loss of the incident ion in the material of the diode, respectively; w is the depletion width of the device, which is assumed in the following to be smaller than the ion penetration range, and L_{diff} is the minority-carrier diffusion length, which is related to the carrier lifetime τ_{min} by $L_{diff} = \sqrt{D_{min} \times \tau_{min}}$, where D_{min} is the diffusion coefficient. The first integral (drift term) represents the contribution from the charge carriers generated within the depletion region and collected as drift current. The second integral (diffusion term) represents the contribution from the minority carriers created in the electroneutral substrate that reach the edge of the depletion region as diffusion current. This simple drift-diffusion model is often used to explain the bias voltage-dependent CCE and to characterize p-n or Schottky junction devices [2, 3, 8]. A basic assumption for the validity of equation (1) is that carrier recombination has to be negligible within the depletion zone, which is fulfilled when the drift times are much shorter than the carrier lifetimes. In that case the measured efficiency should be 100% when the range of the ions is smaller than the depletion thickness (i.e. the CCE only contains the drift term). As will be shown in the next section, this behavior is indeed found for pristine samples, but is not observed in samples irradiated with given proton fluences. In that case, carrier recombination occurs within the active volume of the diodes and the calculation of the CCE using (1) is not accurate. Assume a detector with

parallel-plate geometry, the total induced signal charge Q_s for a packet of charge Q_0 with lifetime τ will be [9]

$$Q = Q_0 \left[\int_0^{t_{cmin}} \frac{\mu_{min} \cdot \mathcal{E}}{w} \cdot e^{-\frac{t}{\tau_{min}}} + \int_0^{t_{cmaj}} \frac{\mu_{maj} \cdot \mathcal{E}}{w} \cdot e^{-\frac{t}{\tau_{maj}}} \right] dt \quad (2)$$

where t_{cmin} and t_{cmaj} are the minority and majority carrier collection times, respectively, $\mu_{min,maj}$ are the corresponding carrier mobility and $\mathcal{E}(x)$ is the applied electric field. The time integrals in (2) can be converted to space integrals using the variable substitution $dt = \pm \frac{dx}{\mu_{min,maj} \mathcal{E}(x)}$. The CCE_{Drift} term then becomes:

$$CCE_{Drift} = \frac{1}{E_i} \int_0^w \frac{dE}{dx} \left[\frac{1}{w} \int_0^x dy e^{-\int_y^x \frac{dz}{L_{min}(z)}} + \frac{1}{w} \int_x^w dy e^{-\int_x^y \frac{dz}{L_{maj}(z)}} \right] dx \quad (3)$$

where $L_{min,maj} = (\mu\tau)_{min,maj} \mathcal{E}(x)$ are the drift lengths. The expression between square brackets simply accounts for the (normalized) probability that a charge carrier created at position x drifts until its respective electrode without being recombined. This probability is identical to the charge collection efficiency profile defined in [2, 10]. The diffusion term has also to be modified to take into account the probability for recombination of the minority carriers originating at $x = w$ and drifting toward the surface electrode.

$$CCE_{Diffusion} = \frac{1}{w} \int_0^w dx e^{-\int_x^w \frac{dz}{L_{min}(z)}} \frac{1}{E_i} \int_w^{R_p} \frac{dE}{dy} e^{-\frac{y-w}{L_{diff}}} dy \quad (4)$$

Equations (3) and (4) describe the drift-diffusion model when carriers can recombine in the depletion and neutral regions. For the case in which the drift lengths are taken to be constant along the path of a given charge carrier, equation (3) becomes the well-known Hecht relation:

$$CCE_{Drift} = \frac{1}{E_i} \int_0^w \frac{dE}{dx} dx \left[\frac{L_{min}}{w} \left(1 - e^{-\frac{x}{L_{min}}} \right) + \frac{L_{maj}}{w} \left(1 - e^{-\frac{w-x}{L_{maj}}} \right) \right] \quad (5)$$

As expected, in the limit when $L_{min,maj} \gg w$ recombination within the depletion region is negligible and equation (5) transforms into the simple drift term. In this work, the 17 MeV protons create a homogeneous vacancy profile through the sample volume [11]. Therefore, the carrier lifetimes will depend only on the irradiated fluence and not on their instantaneous position. As our diodes form a one-sided abrupt junction (Fig. 1), the electric field can be described in first approximation as linearly decreasing from its maximum value at the surface to zero at the edge of the depletion region or at the back contact [9], $\mathcal{E}(x) = \frac{2V}{w^2}(w-x)$, being V the applied bias voltage. We have written a Matlab code to solve equations (3) and (4) for each experimental CCE value using the least square fitting

procedure, where free parameters are the lifetimes for electrons and holes and $L_{min,maj}(x) = (\mu \cdot \tau)_{min,maj} \frac{2V}{w^2} (w - x)$. The mobility and diffusion coefficients are considered to be constant with the accepted values for low field ($\mathcal{E} < 10^4$ V/cm) and low doping concentration ($\mu_e = 1350$ cm²/Vs; $\mu_h = 450$ cm²/Vs; $D_e = 36$ cm²/s; $D_h = 12$ cm²/s). It is worth noticing that due to the particular shape of the $\mathcal{E}(x)$, the exponential term $e^{-\int_x^w \frac{dz}{L_{min}(z)}}$ in equation (4) cancels out. This is because in this simple picture the minority carriers coming from the neutral substrate do not feel any electric field at the junction edge ($x=w$) and they have 100% probability of recombination at this point, so the carriers are never injected into the drift region (in reality, even if $\mathcal{E} = 0$, the carriers would cross the boundary by diffusion). To overcome this mathematical issue, the diffusion term was slightly modified to obtain the probability for a minority carrier to reach the electrode at $x = 0$ starting from $x = 0.95 w$ (i.e. the carrier traverses 95% of the detector):

$$CCE_{Diffusion} = \frac{1}{w'} \int_0^{w'} dx e^{-\int_x^{w'} \frac{dz}{L_{min}(z)}} \frac{1}{E_i} \int_w^{R_p} \frac{dE}{dy} e^{-\frac{y-w}{L_{diff}}} dy \quad (6)$$

where $w' = 0.95 w$.

In order to check the reliability of our model, the data was also analyzed using the recently developed IBIC Simulation Tool (IST) [12], a Monte Carlo approach based on the Shockley-Ramo-Gunn theorem for the simulation of the induced charge pulse and the probabilistic interpretation of the excess charge carrier continuity equations. The program allows interfacing with external electrostatic models, ionization and vacancy density profiles to calculate real-time total and time-resolved charge collection efficiency (CCE) pulses. The IST also provides a model for the carriers' lifetime degradation in irradiated devices, describing the linear decrease in CCE in low damage regime and providing a quantitative description of the radiation hardness parameter according to the model proposed in [13].

Results and discussion

Fig. 3a and 3b show the reverse bias voltage-dependent CCE values for the p and n-type diodes, respectively. The closed dots represent the experimental results while the open symbols are the best fit from our modified drift-diffusion (D-D) model using equations (3) and (6). For the pristine samples, carrier recombination into the drift region is negligible and, therefore, the simulations can only yield a minimum value for the majority carrier lifetime. The lifetime killing effects induced by the 17 MeV proton irradiation is apparent from the decrease of the diffusion length, which in the case of p-type Si drops from 150 ± 30 μm ($\tau_e = 6.5 \pm 2.5$ μs) to 21 ± 2 μm ($\tau_e = 122 \pm 25$ ns) while for n-type Si the worsening is slightly lower, falling from 49 ± 5 μm ($\tau_h = 2.0 \pm 0.4$ μs) to 13.5 ± 1.5 μm ($\tau_h = 152 \pm 40$ ns) after a fluence of 5×10^{12} p/cm². It is important to remark that the fitting of the data for the

irradiated p-type diode using the simple D-D model (not shown) leads to much smaller values ($L_{\text{diff}} = 2.5 \mu\text{m}$; $\tau_e = 2 \text{ ns}$), which demonstrates the necessity to take into account recombination effects within the drift region to perform an accurate analysis of the experimental results.

Recent DLTS studies indicate that a single acceptor state of divacancy, $V_2(-/0)$, is the most abundant defect created after low-dose swift ion implantation in n-type Si [13]. Using the data from Fig 3b we have calculated the probability of divacancy trap production in n-type Si exposed to high energy proton irradiation. From the Shockley-Read-Hall model, the carrier lifetime profile is giving by:

$$\tau(x, \Phi) = \frac{\tau_0}{1 + k \cdot \sigma \cdot \text{Vac}(x) \cdot v_{\text{th}} \cdot \Phi \cdot \tau_0} \quad (6)$$

where τ_0 and $\tau(x, \Phi)$ are the carrier lifetime for the pristine and irradiated material, $\text{Vac}(x)$ is the vacancy profile (≈ 200 vacancies/cm/ion as calculated from SRIM [11]), v_{th} is the thermal velocity ($v_{\text{th}}(e) \approx 2.3 \times 10^7 \text{ cm/s}$; $v_{\text{th}}(h) \approx 1.6 \times 10^7 \text{ cm/s}$), Φ is the particle fluence, k is the average number of electrically active traps per vacancy and σ is the trap cross section. The calculated “effective” trapping cross sections for electrons and holes, defined as the $(k \cdot \sigma)$ product are shown in Table I.

Proton fluence (10^{12} p/cm^2)	$(k \cdot \sigma)_h$ (10^{-16} cm^2)	$(k \cdot \sigma)_e$ (10^{-16} cm^2)
5	3.9 ± 1.2	0.9 ± 0.6
10	4.5 ± 1.1	0.8 ± 0.5

Table I. Calculated values for the effective trapping cross sections for holes and electrons in n-type Si using the S-R-H model.

If we assume the recently published values for the capture cross sections of $V_2(-/0)$ for holes ($\sigma_h = 5 \times 10^{-14} \text{ cm}^2$) and electrons ($\sigma_e = 5 \times 10^{-15} \text{ cm}^2$) [14], the result $k = 0.015 \pm 0.005$ is obtained. This number is considerably smaller than the average value found in [13] ($k = 0.08$, taking $v_{\text{th}}(e) = 2.3 \times 10^7 \text{ cm/s}$), where heavier ions (He, Li, O and Cl) were employed to create the defects. It could be argued that, as SRIM overestimates the number of vacancies because it does not take into account any self-annealing of interstitials and vacancies during the irradiation, this would lead to a smaller value of k . However, the same code was used in [13] to calculate the damage profile, and therefore the k values obtained from both works can be compared. As the density of vacancies produced by those heavier ions is orders of magnitude higher compared to 17 MeV protons, our result suggests that besides direct $V_2(-/0)$ production, the migration and agglomeration of single defects could be an important mechanism for the formation of the divacancies. Moreover, we also have to consider that some of the created electrically active stable defects could have annealed during the elapsed

time between the irradiations and our IBIC measurements (approximately one week) and this could be another reason for getting a lower value of k .

Finally, as stated above, the CCE data was also analysed with the IST Monte Carlo code. In this program, the electrostatics (electric field and weighting potential), ionization and vacancy density profiles are used as inputs, while the free parameters are the $(k \cdot \sigma)$ products for holes and electrons. The obtained results, $(k \cdot \sigma)_h = 2.7 \pm 0.6 \cdot 10^{-16} \text{ cm}^2$ and $(k \cdot \sigma)_e = 0.7 \pm 0.4 \cdot 10^{-16} \text{ cm}^2$, shown in Fig. 4, are in good agreement with those found using our modified D-D model, which reinforce the validity of both methodologies for the analysis of IBIC experiments.

Conclusions

In this paper it has been shown how the simple drift-diffusion model of the CCE can be modified to account for the possibility of carrier recombination within the depletion region. This is fundamental to explain the experimental CCE values found in the case of radiation-damaged detectors and for an accurate extraction of the transport properties of the devices. Our theory has been employed to the study of p and n-type Si diodes irradiated with high energy protons and the results have been confirmed from the parallel analysis using the IST Monte Carlo code.

References

- [1] M. B. H. Breese, P. J. C. King, G. W. Grime, and F. Watt, *J. Appl. Phys.* 72, 2097 (1992).
- [2] M.B.H. Breese, E. Vittone, G. Vizkelethy and P.J. Sellin. *Nucl. Instr. and Meth. B* 264 (2007) 345-360
- [3] N. Iwamoto et al. *IEEE Trans. Nucl. Sci.* 58, No. 1, (2011) 305-313
- [4] T.H. Prettyman. *Nucl. Instr. and Meth. B* 428 (1999) 72-80
- [5] M. B. H. Breese. *J. Appl. Phys.* 74, 3789 (1993)
- [6] G. Vizkelethy, "Annual report of Sandia National Laboratories (SNL) contribution to IAEA CRP F11016" 28 April 2013.
- [7] J. F. Ziegler, J. P. Biersack, and U. Littmark, *The Stopping and Range of Ions in Solids* (Pergamon, New York, 2003)
- [8] M. de Napoli, F. Giacoppo, G. Raciti and E. Rapisarda. *Nucl. Instr. and Meth. A* 608 (2009) 80-85.
- [9] *Semiconductor Detector Systems*. Helmuth Spieler. Oxford University Press.

[10] E. Vittone, IAEA CRP F11016 Technical report, “Modeling of the degradation of charge collection efficiency in detectors subjected to damage ionizing radiation” 2nd May 2012.

[11] J. Garcia Lopez and M.C. Jimenez Ramos Nucl. Instr. and Meth. B 332 (2014) 220-223

[12] J. Forneris, M. Jaksic, Z. Paustovic and E. Vittone. Nucl. Instr. and Meth. B 332 (2014) 257-260

[13] Z. Pastuovic, E. Vittone, I. Capan and M. Jaksic. Appl. Phys. Lett. **98**, 092101 (2011)

[14] L. Vines et al. Phys. Rev. B **79**, 075206 (2009)

Acknowledgements

We thank the members of the IAEA CRP F11016, especially E. Vittone from University of Torino, for useful discussions.

1
2
3
4
5
6
7
8
9
10
11
12
13
14
15
16
17
18
19
20
21
22
23
24
25
26
27
28
29
30
31
32
33
34
35
36
37
38
39
40
41
42
43
44
45
46
47
48
49
50
51
52
53
54
55
56
57
58
59
60
61
62
63
64
65

Figures.

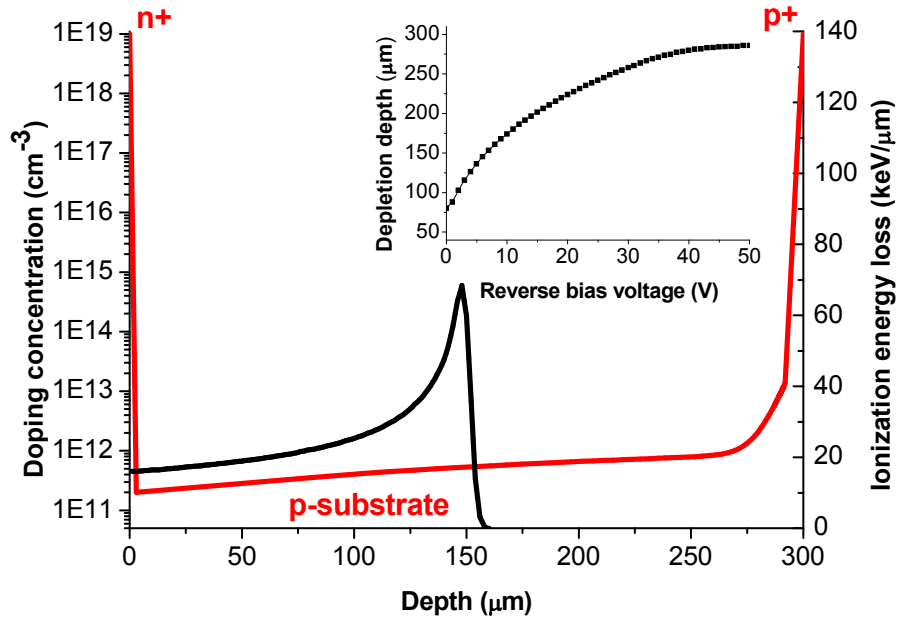
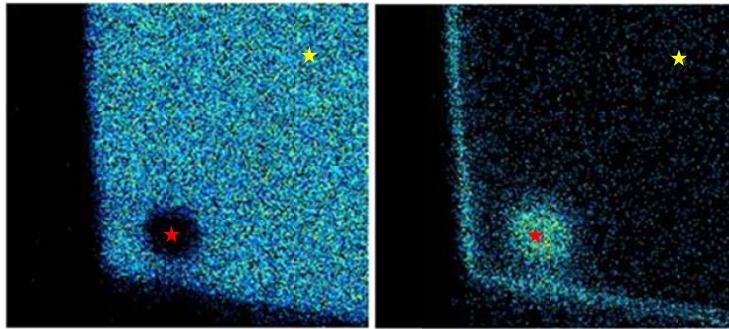


Fig. 1. In red, doping concentration profile of one n⁺-p-p⁺ diode. In black, ionization profile of 4.07 MeV protons in Si. The inset shows the width of the depletion region vs. bias voltage (from [6]).



a) V=30 volts (100-95% CCE) b) V=30 volts (95-90% CCE)

Fig. 2. $1 \times 1 \text{ mm}^2$ IBIC maps recorded around a point irradiated to $1 \times 10^{13} \text{ p/cm}^2$. The damaged spot is clearly visible near the corner of the diode. The red and yellow stars indicate the positions of the point measurements for the irradiated and pristine areas, respectively.

1
2
3
4
5
6
7
8
9
10
11
12
13
14
15
16
17
18
19
20
21
22
23
24
25
26
27
28
29
30
31
32
33
34
35
36
37
38
39
40
41
42
43
44
45
46
47
48
49
50
51
52
53
54
55
56
57
58
59
60
61
62
63
64
65

1
2
3
4
5
6
7
8
9
10
11
12
13
14
15
16
17
18
19
20
21
22
23
24
25
26
27
28
29
30
31
32
33
34
35
36
37
38
39
40
41
42
43
44
45
46
47
48
49
50
51
52
53
54
55
56
57
58
59
60
61
62
63
64
65

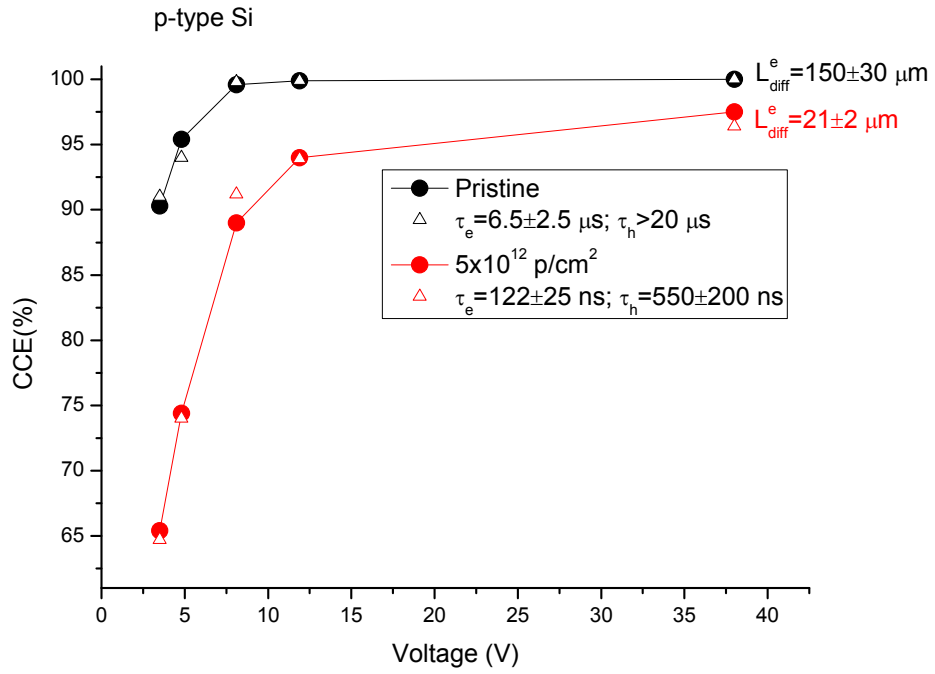


Fig. 3a. Experimental (filled dots) and calculated (open triangles) CCE values using the modified D-D model for pristine (black) and irradiated (red) p-type diodes.

1
2
3
4
5
6
7
8
9
10
11
12
13
14
15
16
17
18
19
20
21
22
23
24
25
26
27
28
29
30
31
32
33
34
35
36
37
38
39
40
41
42
43
44
45
46
47
48
49
50
51
52
53
54
55
56
57
58
59
60
61
62
63
64
65

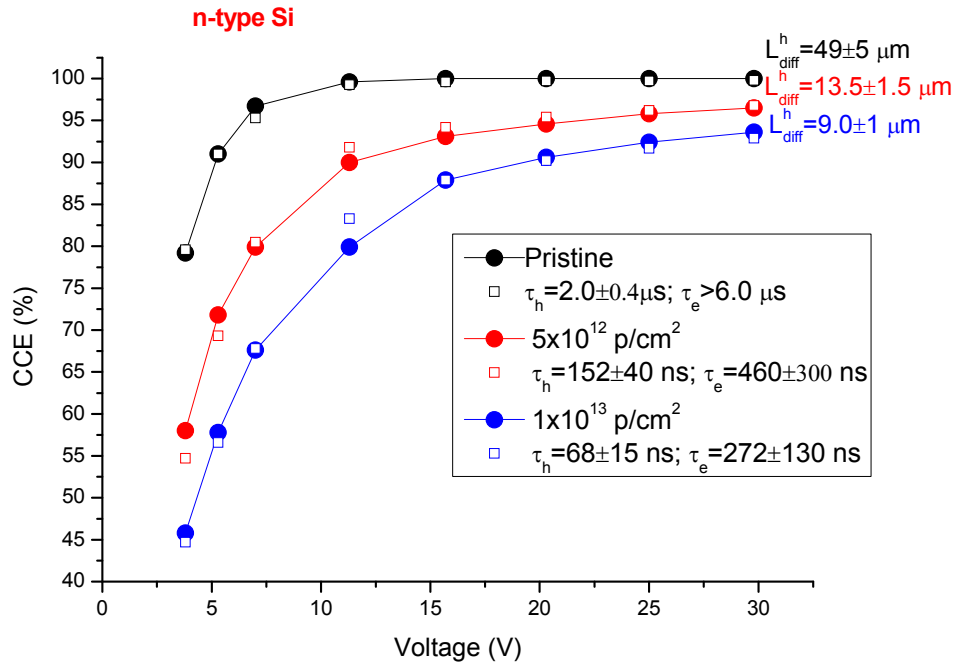


Fig. 3b. Experimental (filled dots) and calculated (open squares) CCE values using the modified D-D model for pristine (black) and irradiated (red, blue) n-type diodes.

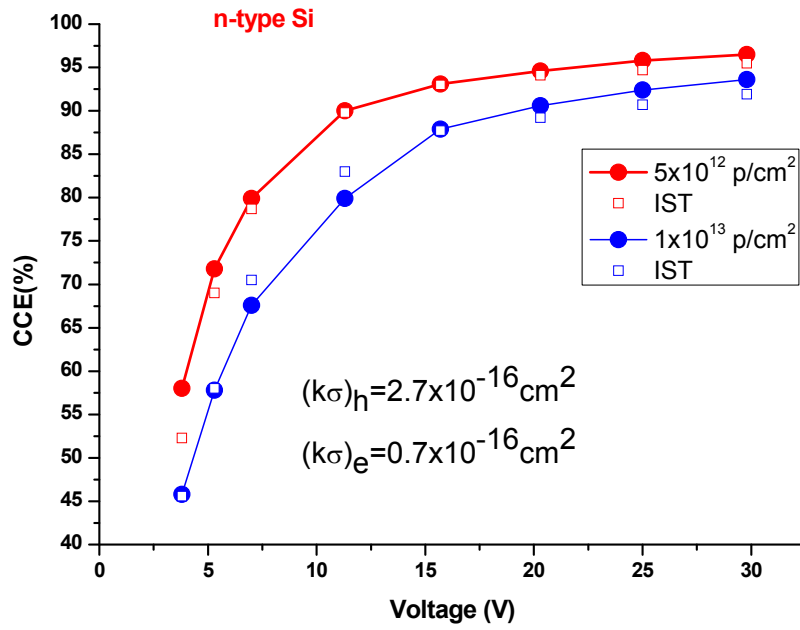


Fig. 4. Experimental (filled dots) and calculated (open squares) CCE values using the Monte Carlo IST code for n-type diodes irradiated at $5 \times 10^{12} \text{ p/cm}^2$ (red) and $1 \times 10^{13} \text{ p/cm}^2$ (blue).